Signal, Image and Video Processing
https://doi.org/10.1007/s11760-018-1286-9

ORIGINAL PAPER

Image dehazing using morphological opening, dilation and Gaussian filtering

Sebastián Salazar-Colores[1] · Juan-Manuel Ramos-Arreguín[1] · César Javier Ortiz Echeverri[1] · Eduardo Cabal-Yepez[2] · Jesus-Carlos Pedraza-Ortega[1] · Juvenal Rodriguez-Resendiz[1]

Received: 16 August 2017 / Revised: 30 January 2018 / Accepted: 11 April 2018

Abstract
Image pre-processing is a critical stage in computer vision systems, with greater relevance when the input images are captured in outdoor environments because the pictures could contain low contrast and modified colors. A common condition present in outdoor images is haze. In this work, a new dehazing algorithm based on dark channel prior mathematical morphology operations (opening and dilation), and a Gaussian filter, is proposed. Moreover, the proposed algorithm performance is compared qualitatively and quantitatively against previously reported algorithms. Obtained results show that the proposed algorithm requires less processing time providing higher quality dehazing results than other state-of-the-art approaches.

Keywords Atmospheric scattering · Contrast enhancement · Dehaze · Dark channel prior · Image enhancement · Image restoration

1 Introduction

Computer vision systems use images as inputs; for this reason, the quality of the images has a direct impact on its performance. An outdoor computer vision system, such as surveillance, autonomous navigation, and remote sensing, assumes that images are acquired in a transparent atmosphere; but in real conditions, the acquired image could be affected by conditions such as inclement weather, haze, fog or smog. These conditions mainly affect the contrast, color, and visibility of the images. Therefore, many image processing algorithms have been created to alleviate such effects. The reduction in these effects is significant for many applications.

In previous works, different approaches have been proposed for dehazing, such as: application of depth information obtained from 3D models of the acquired scene [1], near-infrared information [2], light polarization [3,4], multiple images [5,6], and just a single image. The first four approaches produce excellent results, but their requirements cannot be easily met as is shown in [1,6].

In recent years, the single-image approach has been widely studied, due that most images are captured using common cameras. For instance, Tan maximizes local contrast in the image [7]. Fattal [8] uses the independent component analysis (ICA) to restore the image. He et al. [9] had proposed to use the dark channel prior (DCP) to recover the images with excellent results; however, the main drawback is that the algorithm is expensive in terms of time processing, mainly because of the matting operation used to refine the transmission map (estimation of depth). Since then, many alternatives based on DCP have been proposed to achieve shorter processing times and at the same time good quality; for instance, using image segmentation [10], a guided filter [11], and an edge-guided filter [12], a linear model [13], a median fil-

✉ Juan-Manuel Ramos-Arreguín
jramos@mecamex.net

Sebastián Salazar-Colores
s.salazarcolores@gmail.com

César Javier Ortiz Echeverri
cesarortiz1983@gmail.com

Eduardo Cabal-Yepez
e.cabalyepez@gmail.com

Jesus-Carlos Pedraza-Ortega
caryoko@yahoo.com.mx

Juvenal Rodriguez-Resendiz
juvenal@uaq.edu.mx

[1] Facultad de Informática - Facultad de Ingeniería, Universidad Autónoma de Querétaro, Santiago de Querétaro, Querétaro, Mexico

[2] División de Ingenierías, Campus Irapuato-Salamanca, Universidad de Guanajuato, Salamanca, Guanajuato, Mexico

Published online: 21 April 2018

ter [14], a locally adaptive Wiener filter [15], using a kernel regression model (KRM) on local neighbor data [16], an artificial bee colony [17], or a multiscale product prior [18].

In this research, a DCP-based algorithm is proposed using morphological opening and dilation along with a Gaussian filtering, which is commonly used for image denoising [19], to have a fast and accurate process that creates the transmission map on which the main structures are preserved. The main motivation to use opening and dilation operations is their time performance [20]. The proposed algorithm reduces the processing time drastically in comparison with the original DCP algorithm proposed in [9].

The rest of this paper is organized as follows: in Sect. 2, there is an overview of some concepts upon which the research is based, such as the scattering model, the DCP; in Sect. 3 details of the research process are included. Results compared with two dehazing algorithms from the state of the art are shown in Sect. 4. The conclusion is presented in Sect. 5.

2 Background

The most used atmospheric scattering model in image processing is expressed in Eq. (1) [9]

$$I(\chi) = J(\chi)t(\chi) + A(1 - t(\chi)) \tag{1}$$

where $I(\chi)$ is the image formed for the intensity observed in each of the three R, G or B channels from pixel $\chi = (x, y)$. $J(\chi)$ is the (RGB) image of the original surface of the scene in the real world which corresponds to $\chi = (x, y)$. A is the color vector global airlight. $t(\chi)$ is called transmission which describes the portion of light that reaches the camera. Hence, Eq. (2) based on Eq. (1) shows that to recover the image is necessary to know the variables A and $t(\chi)$.

$$J(\chi) = \frac{I(\chi) - A}{t(\chi)} + A \tag{2}$$

In order to estimate the transmission map $t(\chi)$ and the atmospheric light A, in [9] the dark channel prior (DCP) is proposed, which is an observation over images without haze acquired from outdoors environments. In most local regions of a picture (not representing the sky), at least one color channel (R, G or B) (called dark channel) has a very low intensity in some pixels. In other words, the minimum intensity in such local regions of pixels is a very low value (close to 0). For an image $I(\chi)$, the dark channel is defined as:

$$I^{\text{dark}}(\chi) = \min_{y \in \{r,g,b\}} \left(\min_{c \in (\emptyset)} I^c(y) \right) \tag{3}$$

(a) **(b)** **(c)**

Fig. 1 Result of using a transmission map based on square patches of dark channels, **a** input image, **b** transmission map using dark channel with $\Omega = 15$, **c** recovered image

where $\Omega(\chi)$ is the local patch centered in χ, I^c is the color channel $I(R, G \text{ o } B)$ and y denotes the index for a pixel in $\Omega(\chi)$. In [9] the atmospheric light A is estimated taking from the dark channel map the pixel positions of the 0.1% of the highest intensity values, and from this subset of pixels positions, the pixel in the image $I(\chi)$ with the highest value is assigned as value of A, such as:

$$A = \max \sum_{C=1}^{3} I^C \left[\underset{\chi \in (0.1\% * h * w)}{\arg\max} \left(I^{\text{dark}}(\chi) \right) \right] \tag{4}$$

Moreover, $t(\chi)$ is:

$$t(\chi) = 1 - \min_{y \in \Omega(\chi)} \left(\min_{C \in R,G,B} \left(\frac{I^C(y)}{A^C} \right) \right) \tag{5}$$

Due that the size and shape of the local patch $\Omega(\chi)$ are constant; the recovered image contains non-desirable halos (block effects). In Fig. 1 an example of these halos is shown; however, the proposed method reduces or eliminates these effects on the result.

3 The proposed algorithm

In this paper, an algorithm that estimates a transmission map by computing of the minimal channel [21], morphological opening, Gaussian filter, and morphological dilation, is proposed and depicted in Fig. 2, through a flowchart of the proposed method. In Fig. 3 an example of the stage-by-stage process of the proposed algorithm is observed. Below the process of the proposed algorithm is explained in more detail.

In the proposed algorithm, the estimation of airlight A is performed according to Eq. 4. The input image is normalized according to A (Fig. 3b).

To calculate the transmission $t(\chi)$, the minimal channel of $I(\chi)$ is computed such as is defined in [21] (Fig. 3c):

$$I^{\min}(\chi) = \min_{C \in R,G,B} (I^C(\chi)) \tag{6}$$

Morphological erosion is applied to disappear the small elements in the image's foreground, according to the struc-

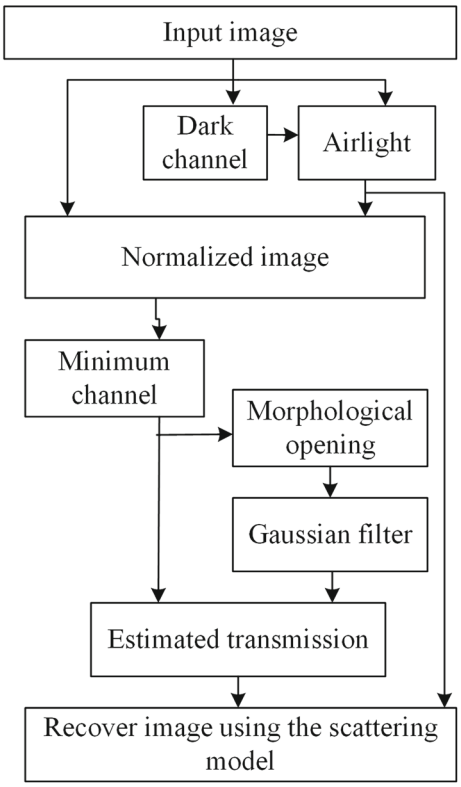

Fig. 2 Flowchart of the proposed algorithm

tural element. In gray-scale images, the operator (ε) is defined in [22] as:

$$[\varepsilon_B(I)](\chi) = \min_{b \in B} I(\chi + b) \tag{7}$$

where B is a structural element centered in χ, formed by pixels b. A morphological dilation (δ) actuate on the picture previously eroded. This operator removes the small elements in the image's background. δ is defined as:

$$[\delta_B(I)](\chi) = \max_{b \in B} I(\chi + b) \tag{8}$$

The application of these two operators is known as morphological opening, and it is mathematically expressed as:

$$\gamma_B(I) = \delta_B[\varepsilon_B(I)] \tag{9}$$

In (Fig. 3d), the result of morphological opening is shown. Posteriorly, a Gaussian filter (GF) is applied [19], as is shown in (Fig. 3e), which smoothes the treated image and removes noise and details, reducing the difference between the squares formed by the opening operation. The Gaussian filtering is performed through the convolution with a mask G, which coefficients are based on an estimation of the distribution:

$$G(x, y) = \frac{1}{2\pi\sigma^2} e^{-\frac{x^2+y^2}{2\sigma^2}} \tag{10}$$

where σ is the standard deviation of the distribution, and (x, y) are the position of the elements of the mask G. Gradients in two adjacent regions are formed as consequence of apply GF. To eliminate them, and at the same time, preserve main structures, dilation (δ) is applied using Eq. (8) (Fig. 3f). Finally, the minimum value between the minimal channel and the result of the dilation is computed to recover the details of the closest elements in the image (Fig. 3g). The proposed algorithm is formally defined by the following pseudo-code.

Algorithm 1 Image dehazing with morphological opening and dilation with Gaussian filtering.

Input: Image $I(x, y)$ with position of pixels $\chi = (i, j)$ where $1 \leq i \leq width(I(\chi))$, and $1 \leq i \leq height(I(\chi))$, a square structural element B_1 to the opening of size s,and to dilate a square structural element B_2 of size d, the Gaussian filter window of size g.
Output: Image $I(\chi)$.

procedure PROPOSEDALGORITHM($I(x, y)$, S_1, S_2, g)
  Estimate the airlight A as in Eq. 4.
  Normalize the image according to A: $I_N(\chi) = \frac{I(\chi)}{A}$.
  Compute the minimal channel as: $I^{min}(\chi) = \min_{C \in R,G,B} (I_N^C(\chi))$.
  Do a morphological opening $I^{\gamma}(\chi) = \gamma_{B_1}(I^{min}(\chi))$.
  Apply a Gaussian filter $I^G(\chi) = GaussianFilter(I^{\gamma}(\chi), g)$.
  Dilate the result of Gaussian filtering $I^D(\chi) = \delta_{B_2}(I^G(\chi))$.
  Estimate the transmission with the minimum value between the inverse of the minimum channel and Gaussian filtering $\bar{t}(\chi) = 1 - \min(I^{min}(\chi), I^D(\chi))$.
  Apply the scattering model $J(\chi) = \frac{I(\chi)-A}{t(\chi)} + A$.
  return $J(\chi)$;
end procedure

4 Experimental results

4.1 Setup

The proposed algorithm was tested with eight images taken from [23], which have been widely used in research works related to dehazing algorithms, to prove and compare its performance. Three of these images, corresponding to real outdoor environments, were used for performing a qualitative analysis, and the remaining five synthetic images were used in order to carry out the quantitative performance comparison, with simulated hazing applying atmospheric scattering model [Eq. 1] with parameters: transmission map ($t(\chi)$) associated with each image, while the atmospheric light $A = [0.8\ 0.7\ 0.9]$ as in [23].

Two popular referenced metrics used in images processing were applied to assess the restoration performance of the proposed algorithm: the MSE (Mean Squared Error), and the SSIM (Structural similarity index) [24]. The MSE (Mean

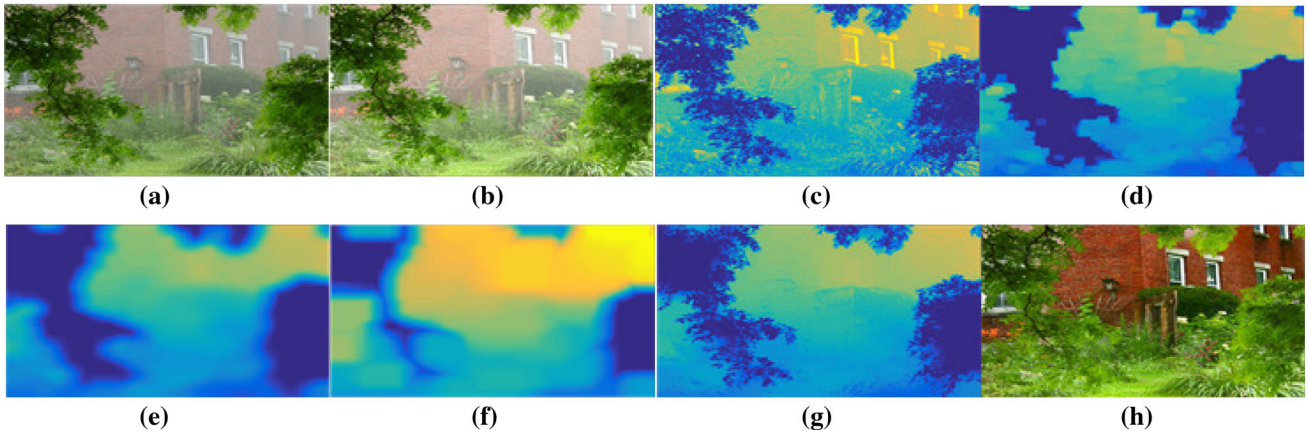

Fig. 3 Example of the algorithm proposed: **a** input image, **b** normalized image, **c** minimal channel, **d** result of morphological opening, **e** result of Gaussian filter, **f** result of morphological dilation, **g** result of compute the minimum of (**c**) and (**f**), **h** recovery image

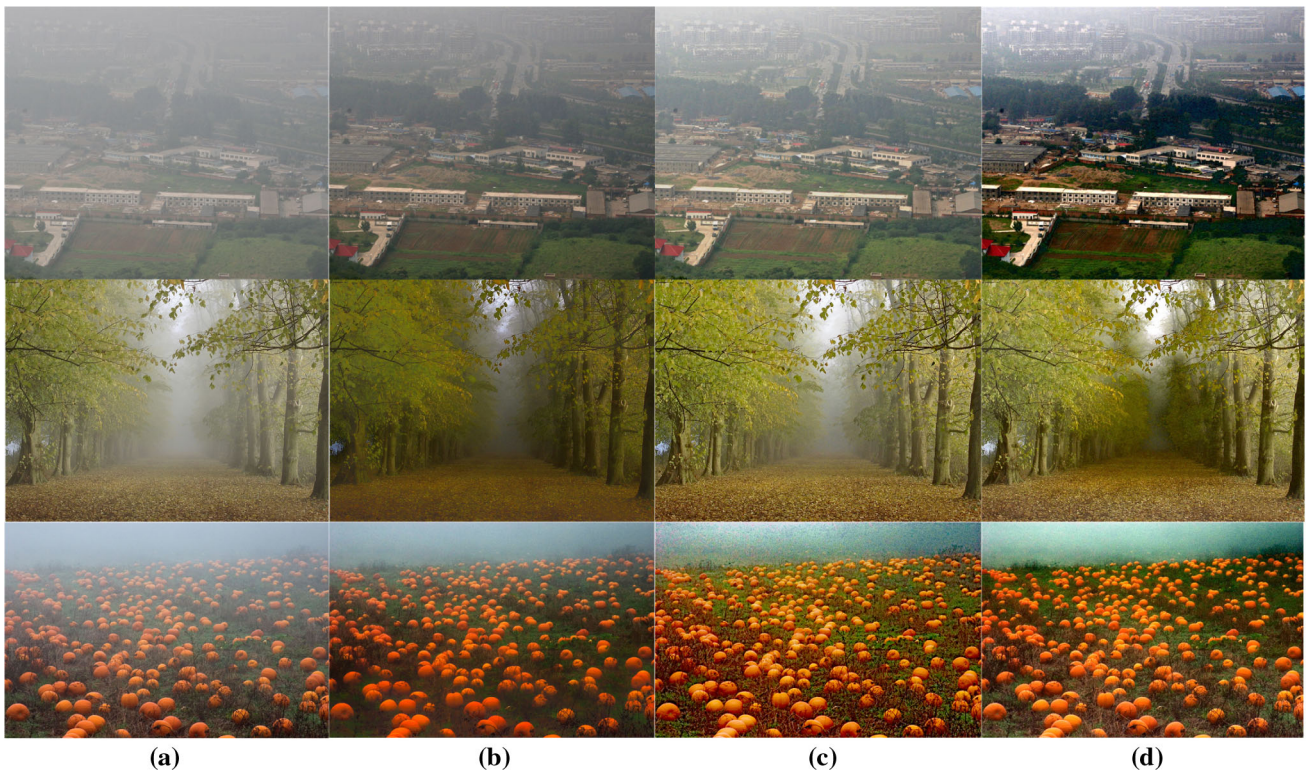

Fig. 4 Results of dehazing algorithms in natural images (canon, forest, pumpkins): **a** input image, **b** Zhu's algorithm [13], **c** Gibson's algorithm [14], **d** proposed algorithm

Squared Error) is defined as:

$$\mathrm{MSE} = \frac{1}{MN}\sum_{y=1}^{M}\sum_{x=1}^{N}[I(x,y) - I'(x,y)]^2 \tag{11}$$

where $I(x, y)$ is the original image, $I'(x, y)$ is the restored version and M, N are the dimensions of the images. A low value for MSE means less error, and consequently a better performance in the restoration. On the other hand, the SSIM, which is a normalized metric based on a perception-based model, is defined as:

$$S(x,y) = f(l(x,y), c(x,y), s(x,y)) \tag{12}$$

where $l(x, y)$ is the luminance comparison, $c(x, y)$ is the contrast comparison, and $s(x, y)$ is the structure comparison.

The optimal parameters of the algorithm were determined experimentally. The size s for the structural element B_1 is:

Fig. 5 Results of dehazing algorithms in synthetic images (bikes, roofs2, trees2): **a** input image, **b** ground-truth image, **c** Zhu's algorithm [13], **d** Gibson's algorithm [14], **e** proposed algorithm

15, the size d for the structural element B_2 is: 42, the size of the Gaussian filter g is: 37.

The performance of the proposed algorithm is compared against two state-of-the-art approaches, the Gibson et al. in [14], which uses a technique for refining the transmission by modifying the Dark channel prior through the Median dark channel, and Zhu et al. in [13] that proposes an algorithm based on a prior linear color attenuation, and the difference between the brightness and the saturation of the pixels within the hazy image. The parameters used in the implemented algorithms were proposed by their corresponding authors. A kernel size of 11×11 and a $\omega = 0.95$ were used for Gibson et al. [14], whereas $\Omega(\chi) = 15$, a $\beta = 0.8$ and $\omega = 0.95$ were used for Zhu et al. [13]. The experimentation was performed in a PC with an $i5$ 3320 CPU @2.60 GHz and 4 GB RAM, using $C++$ and the $OpenCV$ library.

4.2 Qualitative analysis

Figure 4 shows a qualitative comparison of results of Gibson et al. [14] and Zhu et al. [13], and the propose approach, with three natural images (canon, forest and pumpkins). Most of the haze is removed through the three algorithms. However, it can be observed that the proposed method recovers a better contrast and colors than the other two techniques in canon image. From the forest image, it can be appreciated that the Zhu et al. result presents a worse color contrast those form Gibson et al. and our proposed algorithm, although little halos can be observed. In the pumpkins image, the proposed method presents better representation of the sky, and non-saturated colors differ from the other two approaches.

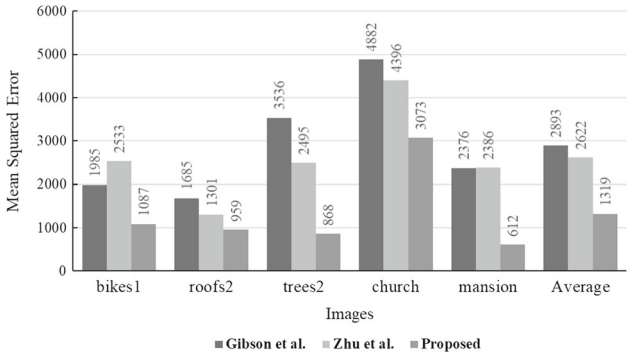

Fig. 6 Comparison of the structural similarity (SSIM) index for the different algorithms

4.3 Quantitative analysis

In Fig. 5, the results of applying dehazing algorithms in synthetic images are shown. Figures 6 and 7 show bar plots that represent the results of evaluating the proposed algorithm, Zhu et al. [13] and Gibson et al.[14] through SSIM and MSE metrics, respectively. From these figures it is clear that the proposed algorithm outperforms the other two for all the treated images in both metrics. Figure 8 presents a processing-computational time comparison for a 600×400-pixels image, showing that the proposed algorithm is at least one order of magnitude faster than the other algorithms.

5 Conclusions

Qualitative analysis in outdoor-hazing images suggests that the proposed algorithm enables us to obtain more background

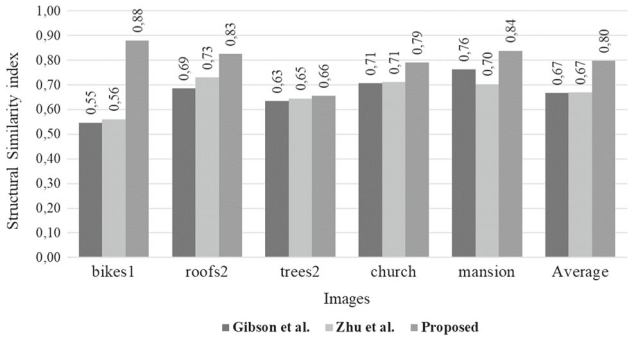

Fig. 7 Comparison of the mean squared error (MSE) index for the different algorithms

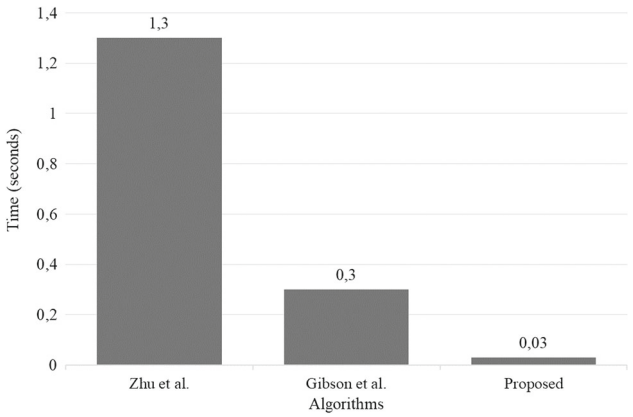

Fig. 8 Comparison of processing time for a 600 × 400 pixels image in the different algorithms

details in comparison with two state-of-the-art methods. Furthermore, a quantitative analysis using SSIM and MSE metrics was carried out over different synthetic images, which indicates that the proposed algorithm is more precise than the considered approaches. Nevertheless, the main contribution of this work is related to the low-time processing achieved through the combination of mathematical morphology, Gaussian filtering and dark channel calculations, which are by themselves low-computing complexity algorithms. This advantage could be exploited on video dehazing, opening possibilities in artificial vision such as automatic navigation, surveillance systems, and optical inspection of industrial processes in contaminated environments, among many others.

Acknowledgements Sebastián Salazar-Colores wants to thank CONACYT (Consejo Nacional de Ciencia y Tecnología) for the financial support of his Ph.D. studies.

References

1. Kopf, J., Neubert, B., Chen, B., Cohen, M., Cohen-Or, D., Deussen, O., Uyttendaele, M., Lischinski, D.: Deep photo: model-based photograph enhancement and viewing. ACM Trans. Graph. (TOG) **27**(5), 116:1 (2008)
2. Schaul, L., Fredembach, C., Susstrunk, S., Süsstrunk, S.: Color image dehazing using the near-infrared. In: IEEE International Conference on Image Processing (ICIP), Cairo, Egypt, vol. 1, pp. 1629–1632 (2009). https://doi.org/10.1109/ICIP.2009.5413700
3. Liu, Q., Zhang, H., Lin, M., Wu, Y.: Research on image dehazing algorithms based on physical model. In: International Conference on Multimedia Technology (ICMT), Hangzhou, China, vol. 2, pp. 467–470 (2011). https://doi.org/10.1109/ICMT.2011.6003078
4. Wang, X., Jin, X., Xu, G., Xu, X.: A Multi-scale decomposition based haze removal algorithm. In: International Conference on Remote Sensing, Environment and Transportation Engineering (RSETE), Nanjing, China, vol. 2, pp. 1–4 (2012)
5. Carr, P., Hartley, R.: Improved single image dehazing using geometry. In: Digital Image Computing: Techniques and Applications (DICTA), Melbourne, Canada, vol. 1, pp. 103–110 (2009). https://doi.org/10.1109/DICTA.2009.25
6. Schechner, Y.Y., Narasimhan, S.G., Nayar, S.K.: Instant dehazing of images using polarization. In: IEEE Computer Society Conference on Computer Vision and Pattern Recognition (CVPR), Kauai, USA, vol. 16, pp. I-325 (2001)
7. Tan, R.T.: Visibility in bad weather from a single image. In: IEEE Conference on Computer Vision and Pattern Recognition (CVPR), Anchorage, USA, vol. 1, pp. 1–8 (2008)
8. Fattal, R.: Single image dehazing. In: ACM Transactions on Graphics (TOG), New York, USA, vol. 27, pp. 72:1–72:9 (2008). https://doi.org/10.1145/1360612.1360671
9. He, K., Sun, J., Tang, X.: Single image haze removal using dark channel prior. IEEE Trans. Pattern Anal. Mach. Intell. **33**(12), 2341 (2010). https://doi.org/10.1109/TPAMI.2010.168
10. Fang, S., Zhan, J., Cao, Y., Rao, R.: Improved single image dehazing using segmentation. In: IEEE International Conference on Image Processing (ICIP), Hong Kong, China, vol. 1, pp. 3589–3592 (2010). https://doi.org/10.1109/ICIP.2010.5651964
11. Pang, J., Oscar, A., Zheng, G.: Improved single image dehazing using guided filter. In: Proceedings of the APSIPA Annual Summit and Conference (APSIPA ASC), Xi'an, China, vol. 1, pp. 1–4 (2011)
12. Zhu, X., Li, Y., Qiao, Y.: Fast single image dehazing through Edge-Guided Interpolated Filter. In: International Conference on Machine Vision Applications (MVA), Tokyo, Japan, vol. 1, pp. 443–446 (2015). https://doi.org/10.1109/MVA.2015.7153106
13. Zhu, Q., Mai, J., Shao, L.: A fast single image haze removal algorithm using color attenuation prior. IEEE Trans. Image Process. **24**(11), 3522 (2015). https://doi.org/10.1109/TIP.2015.2446191
14. Gibson, K.B., Võ, D.T., Nguyen, T.Q.: An investigation of dehazing effects on image and video coding. IEEE Trans. Image Process. **21**(2), 662 (2012). https://doi.org/10.1109/TIP.2011.2166968. http://ieeexplore.ieee.org/stamp/stamp.jsp?tp=&arnumber=6008642&isnumber=6129825. Accessed 15 Feb 2017
15. Gibson, K.B., Nguyen, T.Q.: Fast single image fog removal using the adaptive Wiener filter. In: 2013 IEEE International Conference on Image Processing, vol. 1, pp. 714–718. IEEE, Melbourne, Canada (2013). https://doi.org/10.1109/ICIP.2013.6738147. http://ieeexplore.ieee.org/document/6738147/
16. Xie, C.H., Qiao, W.W., Liu, Z., Ying, W.H.: Single image dehazing using kernel regression model and dark channel prior. Signal Image Video Process. **11**(4), 705 (2017). https://doi.org/10.1007/s11760-016-1013-3
17. Akay, B., Karaboga, D.: A survey on the applications of artificial bee colony in signal, image, and video processing. Signal Image Video Process. **9**(4), 967 (2015). https://doi.org/10.1007/s11760-015-0758-4
18. Kaplan, N.H., Ayten, K.K., Dumlu, A.: Single image dehazing based on multiscale product prior and application to vision control.

Signal Image Video Process. **11**(8), 1389 (2017). https://doi.org/10.1007/s11760-017-1097-4
19. Deng, G., Cahill, L.W.: An adaptive Gaussian filter for noise reduction and edge detection. In: IEEE Conference Record Nuclear Science Symposium and Medical Imaging Conference, vol. 3. pp.1615–1619. San Francisco, USA, (1993). https://doi.org/10.1109/NSSMIC.1993.373563. http://ieeexplore.ieee.org/stamp/stamp.jsp?tp=&arnumber=373563&isnumber=8547
20. Vincent, L.: Morphological grayscale reconstruction in image analysis: applications and efficient algorithms. IEEE Trans. Image Process. **2**(2), 176 (1993)
21. Li, Z., Zheng, J., Yao, W., Zhu, Z.: Single image haze removal via a simplified dark channel. In: IEEE International Conference on Acoustics, Speech and Signal Processing (ICASSP), South Brisbane, Australia, vol. 1, pp. 1608–1612 (2015). https://doi.org/10.1109/ICASSP.2015.7178242
22. Soille, P.: Morphological Image Analysis: Principles and Applications. Springer, Berlin (2013)
23. Fattal, R.: Dehazing using color-lines. ACM Trans. Graph. (TOG) **34**(1), 13:1 (2014). https://doi.org/10.1145/2651362
24. Dosselmann, R., Yang, X.: A comprehensive assessment of the structural similarity index. Signal Image Video Process. **5**(1), 81 (2011). https://doi.org/10.1007/s11760-009-0144-1